

A.P.N. Sutherland

Aeroelasticity Facility
 Division of Aeronautical Systems Technology,
 Council for Scientific and Industrial Research
 Pretoria, RSA

ABSTRACT

As an on-going exercise to establish an experimental aeroelastic capability, the design of a 0,21 Mach scaled (reduced stiffness) cantilever wing was undertaken, for testing in the new National Medium Speed Wind Tunnel. Described are the choice of scaling factors, estimation of full scale properties, materials evaluation, sizing and construction of the first (calibration) model and calibration procedures to be followed. At all times an effort was made to maintain simplicity in the model design, whilst imposing the limitations of available materials and construction methods. Some preliminary calibration results from the completed model are presented, which indicate good simulation of the full scale wing.

NOMENCLATURE

BM	- bending moment.
E	- elasticity modulus.
EI,GJ	- bending and torsional stiffness.
F	- forces.
FE	- finite element.
Fr	- Froude number.
G	- shear modulus.
GVT	- ground vibration test.
h	- altitude.
I'	- mass inertia.
l	- length.
M	- Mach number.
m	- mass, mass/length.
p _{to}	- stilling chamber pressure.
q	- dynamic pressure.
Re	- Reynold's number.
Str	- Strouhal number.
t	- thickness, time.
UD	- unidirectional.
u	- displacement.
V	- velocity.
γ	- ratio of specific heats.
δ	- damping.
Δ	- linear deflection.
μ	- mass density ratio.
ν	- Poisson's ratio.
ρ	- density.
ω	- frequency (rad/sec).

Subscripts; Superscripts:

a	- aircraft.
m	- model.
o	- reference value.
r	- ratio (m/a).
11,22,12	- denote in-plane properties.
() ^T	- transpose

INTRODUCTION

The capability currently exists within DAST to perform analytical sub- or supersonic flutter predictions for complete aircraft configurations. Unsteady generalised forces are obtained analytically, whilst modal information comes from finite element modelling or ground vibration testing. To expand on this capability, and provide experimental backup for the calculations, a project was initiated to develop flutter and unsteady pressure measurement wind tunnel models, for testing in the new National Medium Speed Wind Tunnel. The value of flutter models in assessing design or configuration changes with regard to flutter boundaries, or new designs prior to prototype flight testing, is well known. Described here is the initial attempt to develop an in-house flutter modelling capability which will ultimately enable comprehensive wind tunnel flutter testing.

The main aim was to gain a thorough understanding of the principles and requirements of flutter model design, construction and testing, using relatively simple and cheap models. This in turn would ensure a good foundation on which to base future efforts. The task of establishing this basic modelling technology was split into two phases, the first of which (now completed) comprised a training exercise employing a generic low speed model. The second phase of the project involves the design, construction and testing of a Mach scaled cantilevered wing. The design and construction of the model are described in this paper.

To ease design and manufacture problems, and because of high selected tunnel q values, this model is of reduced stiffness and large size. Model semi-span, including a tip store, was set at 65% of the tunnel width. This is much larger than is generally used for transonic cantilever models, but was chosen as the model is for training purposes and the gathering of qualitative data only. Outlined below is the design approach used in developing the first (calibration) model, including scaling factors, determination of full scale properties, choice of model materials, sizing of model components, construction of the model and proposed calibration procedures to check its validity. Some preliminary calibration results are presented.

In designing the model an effort was made to maintain structural simplicity, whilst imposing the limitations of available materials and construction techniques. Less use was made of finite element modelling than originally envisaged. It is expected though, that the finite element model (of the physical model) will come into its own once full calibration results

of this first sample are available. These will enable final updating, after which the finite element model will prove useful in evaluating design changes to be incorporated in the second (improved) tunnel test model, as well as in parametric studies prior to tunnel testing.

PROJECT OBJECTIVES

The major goals of this part of the project were to:

- Develop the expertise to design and construct fibre composite Mach scaled models to represent full scale metal structures.
- Set up the procedures for detailed calibration of the models to check their validity.
- Based on calibration results and an understanding of the physics, perform any model redesign required to ensure proper matching of the full scale structure.

STRUCTURE SELECTED FOR SCALING

The structure selected for this exercise is a shoulder mounted wing, with 5° anhedral from the root, 47°30' sweepback on the leading edge and an extended chord on approximately the outer two-thirds of the semi-span. Its construction is essentially an all metal two spar torsion box structure, with intermediate lighter gauge spars. The variable thickness skin provides almost all the bending stiffness. There are two differentially operated, double slotted flaps and an aileron on the trailing edge. The leading edge has a flap inboard and a slat outboard. Two spoilers are located on the wing, between the rear spar and the flaps. Figure 1 illustrates the geometry of the clean wing, showing pertinent dimensions and the coordinate reference axes.

SCALE FACTORS FOR MACH SCALING

The first step in the design of a flutter model is to establish applicable scaling factors. To ensure true similitude for a model of this nature (a flexible body experiencing unsteady motion in a compressible flow in a gravity field)

$$(Re, M, \gamma, Str, Fr, \mu, \delta)_m = (Re, M, \gamma, Str, Fr, \mu, \delta)_a \quad (1)$$

Eqn. (1) represents severe requirements which cannot be met in practice. For Mach scaled models the requirements on Re, Fr and δ can be relaxed, and small variations in γ are acceptable. It is necessary only to (a) ensure similar support, frequencies and mode shapes, (b) have similar aerodynamic (geometric) shape and (c) have similar compressible flow patterns (M) to the full scale structure. Thus Eqn. (1) reduces to

$$(M, Str, \mu)_m = (M, Str, \mu)_a \quad (2)$$

The aircraft flight point selected for scaling was

$$h_a = 2000 \text{ m} ; M_a = 0,95 \Rightarrow q_a = 50260 \text{ N/m}^2 \quad (3)$$

and the selected model design point was

$$p_{to} = 150 \times 10^3 \text{ N/m}^2 ; M_m = 0,95 \quad (4)$$

Assuming isentropic flow in the tunnel, and taking $\gamma_{air} = 1,4$ then by Eqn. (4)

$$q_m = p_{to} \left[\frac{0,7 M_a^2}{(1 + M_a^2/5)^{3,5}} \right] = 53016 \text{ N/m}^2 \quad (5)$$

The length scale factor was fixed by selecting the model semi-span (4,623 m with tip store) to be 65% of tunnel width (1,50 m). Thus

$$l_r = (0,65)(1,50/4,623) = 0,21 \quad (6)$$

To ease design and manufacture problems for this first attempt, a model of reduced stiffness was decided on. This means that the flutter margin (on velocity) is built into the model, so testing need not go beyond the tunnel design point. This margin is included by specifying the model reduced frequency to be lower, by the speed margin, than that of the full scale structure. A 20% speed margin was chosen, so at the model design point, Eqn. (2) becomes

$$\left. \begin{aligned} \mu_m &= \mu_a \\ (V/l\omega)_m &= 1,20(V/l\omega)_a \\ M_m &= M_a \end{aligned} \right\} (7)$$

Using Eqns. (3) to (7) scaling factors were derived as:

$$\left. \begin{aligned} q_r &= q_m/q_a &= 1,05482 \\ V_r &= a_r &= 0,9826 \\ \rho_r &= q_r(1/V_r)^2 &= 1,0925 \\ m_r &= \rho_r l_r^3 &= 0,010118 \\ I_r' &= \rho_r l_r^5 &= 0,4462 \times 10^{-3} \\ \omega_r &= V_r/(1,20 l_r) &= 3,8992 \\ EI_r &= GJ_r = (1/1,20)^2 q_r l_r^4 &= 1,4246 \times 10^{-3} \\ F_r &= q_r l_r^2 &= 46,518 \times 10^{-3} \\ BM_r &= q_r l_r^3 &= 9,7687 \times 10^{-3} \\ \Delta_r &= (1,2)^2 l_r &= 0,3024 \end{aligned} \right\} (8)$$

PROPERTIES TO BE SCALED

Full scale structural data to be scaled is usually provided by the manufacturer to the model designer. In this case, with the exception of a reasonable mass distribution, such information was not available and had to be determined analytically or experimentally. To obtain the necessary elastic and dynamic characteristics of the wing, the following were done:

- From structural drawings area properties and shear centre locations along the semi-span were calculated using a program SECP⁽¹⁾.
- Ground vibration tests (GVT's) of the full scale, equipped cantilevered wing, clean and with tip store.
- GVT's of the launcher and tip store, individually and connected, as free-free beams.
- Comprehensive static loading tests, designed to simulate first and second bending and torsion mode shapes, and to check linearity.

Mass Distribution

The mass distribution provided specified 40 chord-wise and spanwise bays, each with a given mass and centre of gravity location. Pitch, roll and yaw inertias, and overall wing centre of gravity, with respect to given reference axes, were also supplied.

Mass distributions for the launcher and store were not provided, but the total mass, centre of gravity location and inertia of each was measured. This together with GVT results for these components, was adequate for model design purposes.

Structure Sectional Properties

Measured wing mode shapes indicated that in the frequency range of interest the wing structural box exhibits little chordwise bending. In view of this, cross sectional properties were calculated at 26 spanwise stations, selected such that changes in section, skin thickness, spar sizes etc. were included.

Properties calculated were (a) for the complete structure: EI_x , EI_y , GJ and shear centre position and (b) for the skin only: EI_x and EI_y . Skin only calculations were done to determine the relative contribution of the skin to the total wing bending stiffness, in order to preserve the correct balance (skin to internal structure) in the model. In evaluating these properties, only the main structural box was considered. Leading and trailing edge control surfaces were assumed to contribute nothing to wing stiffness. All the calculations were done using the program SECP. Prior to its use, SECP was checked against analytical and finite element solutions, and found to be accurate in this application. Figure 2 shows the calculated properties, after scaling to model target values.

Wing Ground Vibration Test

Ground vibration tests were done on the wing, which was cantilevered "rigidly" from a massive, reinforced concrete block, for both clean wing and tip store configurations. Hydraulic pressure was applied during the tests to maintain the correct control surface/wing connection stiffnesses. For the clean wing configuration five modes were isolated, while for the tip store configuration the first eight modes were obtained. Only the modes of relevance in the model design were considered further. This effectively excluded modes with significant control surface contributions, as control surfaces were not to be included in the model. Tables 1 and 2 and Figures 3 and 4 give modes of interest.

Launcher and Store Ground Vibration Tests

Simple ground vibration tests were done on launcher and store, both individually and as a unit. In each case, the "structure" was suspended on soft elastics, such that the free-free rigid body modes of the system occurred below 2 Hz. Only the first bending modes (transverse and in-plane for the launcher, transverse for the axi-symmetric store) were considered relevant, based on deflected shapes observed during the wing plus store GVT. Typical free-free first bending mode shapes were measured. Their frequencies are given in Table 3.

Wing Static Load Tests

To obtain static deflection data which could later be used as a check on both the finite element and physical model stiffness distributions, various combinations of bending and twisting loads were imposed on the wing. These tests were designed to simulate first and second bending and torsion deflection shapes. It was attempted to load the wing in pure bending or pure torsion (about the "elastic axis") as the case may be, but in practice this was difficult, and resulted in some data that was difficult to interpret.

These tests were done with the wing mounted exactly as for the GVT's. Obviously this mounting was not "rigid". To account for this, the deflections of laser beams reflected from small mirrors located both on the wing root and the backstop, in spanwise and chordwise (equivalently bending and torsion) directions were measured. These allowed "rigid body motion" to be subtracted out of the measured deflections, to leave only the desired elastic deformations. Loads were applied to

the wing by hydraulic jacks, via rectangular steel frames, and were measured with tensile force transducers located between the jacks and the frames. All deflections were measured with mechanical dial gauges. This arrangement was not entirely satisfactory, but was all that could be done within cost and time constraints. In spite of this the results obtained are considered reliable.

For each full test, measurements were made at zero load, half load and full load, in both loading and unloading directions. For the linearity checks, smaller load increments were used. The results obtained showed a small amount of hysteresis, but were effectively linear (within the scatter band). The root mounting was shown to be essentially rigid torsionally, but flexible in bending, resulting in a maximum "rigid body" bending deflection at the wing tip of $\Delta \approx 5,8$ mm.

The results of all the torsion load cases were difficult to interpret, and showed more non-linearity than bending results. This was probably due mainly to applied loads being asymmetrical about the "elastic axis", and too low. Due to wing sweep, there were bending and torsional contributions to the measured deflections, which could not be "decoupled". Torsional deflections were small ($\sim 1/10$ bending deflections), so the relative error in reading them was much larger than for the bending cases.

Measured static deflections were used in two ways:

- (a) Directly, by comparison with measured model deflections, after appropriate scaling. Figure 5 illustrates this use. In this figure, deflections for points 19 and 21 (see Figure 9), after correction for root end flexibility, are shown for a tip bending case.
- (b) To calculate stiffness terms relating loading and measurement points. In this case surface splines were fitted to obtain deflections at all desired points, after which an under- or over-determined system of equations was solved (once for each set of load cases), for stiffness terms relating the load-load and load-deflection points. Q-R decomposition was used after appropriate re-organisation of the matrices (forces and deflections) to the form

$$(Ax)^T = (y)^T \quad (9)$$

where A = flexibility matrix ($l \times n$)
 x = force matrix ($n \times m$)
 y = deflection matrix L ($l \times m$)

The idea behind this approach was to do the same calculations with model and FEM results, thus enabling direct comparison of the stiffnesses of load paths, hence identification of too stiff or too soft areas in the model. Software to do this was developed, using LINPACK routines⁽²⁾. It is felt that in practice direct comparison of deflections will be more useful.

MODEL PRELIMINARY DEFLECTION ANALYSIS

Calculation of Steady Loads

Steady loads on the model at the design conditions were calculated using USTORE, for both clean wing and tip store configurations⁽³⁾. USTORE is based on linearised potential flow, so the solution for a given Mach number is linear with respect to incidence. Calculations were made at two incidence values, $\alpha = 0^\circ$ and $\alpha = 5^\circ$. Loads at intermediate α values were found by

interpolation and compressibility effects were included via the Göthert Rule (a limitation of USTORE). Free stream conditions were

$$M_{\infty} = 0,95 \quad ; \quad q_{\infty} = 53016 \text{ N/m}^2 \quad (10)$$

The results were obtained in two forms, (a) as loads and moments on each strip of the aerodynamic model and (b) as static pressures on both upper and lower surfaces of the wing.

Model Deflections

The purpose of the steady load calculations was to check model deflections at the design point. Excessive deflections would indicate the need to build the model in a "jig shape", such that its deflected shape at the test point was correct. To do this, a simple beam FE model was made, as depicted in Figure 6. Beam stiffnesses used in the analysis were scaled from full scale calculated values. For the maximum load case ($\alpha = 2^\circ$, tip store on) aerodynamic loads were transferred to structural node points and wing tip deflections were calculated as:

$$\begin{aligned} \text{Bending deflection at point 20} &= 25,1 \text{ mm} \\ \text{Rotation (twist) at point 20} &= 0,8^\circ \end{aligned}$$

This model was also used to check the effect of changing the stiffnesses of beams 2 and 3 (Figure 6). A variation of 30% changed calculated tip deflections by ~6% (bending) and ~2,5% (torsion). This indicated that the model was not very sensitive to root rib stiffness, thus easing modelling requirements in this area. Calculated deflections were not excessive, so it was decided not to use a "jig shape" in the design and construction of the model.

MODEL DESIGN

The basic design problem was to develop a fibre-composite material model structure that elastically and dynamically represented the full scale metal wing, for clean wing and wing plus tip store configurations. The primary design criterion was to match the first three to five natural modes of the full scale structure for each configuration respectively, whilst simultaneously providing sufficient strength to support the expected steady and dynamic loads at the test condition.

The resulting model is a half-span model with a ballasted mass of 6,587 kg, a semi-span of 0,886 m from the fuselage centre line, a root chord (projected to fuselage centre line) of 0,985 m, and a tip chord of 0,281 m. Thus taper ratio is 0,285 and aspect ratio (based on semi-span) is 1,400. The external geometry of the model follows that of the full scale wing, except for control surface details. All control surfaces were excluded from this first model.

Finite Element Model

To support the model design a finite element (FE) model of the physical model was developed at an early stage, using PERMAS⁽⁴⁾ and currently has 674 nodes, 862 elements (quadrilateral and triangular) and 12 "materials". Due to problems encountered in using and verifying previously untried elements⁽⁵⁾ (within DAST), the FE model was not used in the design iterations as much as originally intended. Orthotropic and/or layered shell elements, in which bending and membrane or membrane only actions are switchable, were used for skin and stiffener representation.

The FE model can now be used for both static and dynamic analysis, but needs improvement in the following areas, (a) inclusion of spar caps as necessary, (b) introduction of proper skin offsets, (c) more detailed representation of the main root attachment and (d) improved representation of mass properties.

The preliminary model analysis yielded a good, but in places complicated structure. Based on the calibration results of the first model, the FE model will be updated and used extensively in the redesign process to ensure a good final structural design.

It is intended to use substructuring techniques to analyse different pylon/store combinations, which in turn will allow parametric flutter studies prior to wind tunnel testing.

Choice of Materials and Material Properties

Due to limitations in fabrication techniques available within DAST, the model structure had to be kept simple. It was therefore decided to use carbon composites, birch plywood and polyester foam (60 kg/m³) as much as possible, with metal fittings as necessary. Carbon fabrics TORAYCA 6104 (UD hybrid) and 6142 (balanced weave) were selected as they were the thinnest available (0,15 mm), a desirable feature in that it allowed greater flexibility in model skin design. These fabrics had not been used at DAST before, so basic material properties had to be established. Vacuumed (at 80%) test coupons were made, and the following quantities determined:

$$\begin{aligned} \text{TORAYCA 6104/EPO 625} \\ \left. \begin{aligned} E_{11} &= 83,9 \text{ GPa}, E_{22} = 11,9 \text{ GPa}, G_{12} = 5,41 \text{ GPa} \\ \nu_{12} &= 0,295 \\ S_{11} &= 950 \text{ MPa} \\ \text{Fibre volume fraction} &= 0,50 \end{aligned} \right\} (11) \end{aligned}$$

$$\begin{aligned} \text{TORAYCA 6142/EPO 625} \\ \left. \begin{aligned} E_{11} = E_{22} &= 41,6 \text{ GPa}, G_{0/90} = 3,50 \text{ GPa} \\ \nu_{12} = \nu_{21} &= 0,109 \\ S_{11} &= 390 \text{ MPa} \\ \text{Fibre volume fraction} &= 0,50 \end{aligned} \right\} (12) \end{aligned}$$

The full scale wing is constructed of aluminium, for which

$$\left. \begin{aligned} E &= 72,5 \text{ GPa}, G = 27,6 \text{ GPa}, \nu \approx 0,313 \\ S &= 460 \text{ MPa} \end{aligned} \right\} (13)$$

The quasi-isotropic (minimum expected) properties of candidate laminates were estimated using the following equations⁽⁶⁾

$$\left. \begin{aligned} \bar{E}_x &\approx \bar{E}_y \approx 0,375 E_{11} + 0,625 E_{22} \\ \bar{G}_{xy} &\approx 0,125 E_{11} + 0,25 E_{22} \end{aligned} \right\} (14)$$

For TORAYCA 6104/EPO 625, the material used for the wing skins, Eqns. (11) and (14) give

$$\left. \begin{aligned} \bar{E}_x = \bar{E}_y &= 38,9 \text{ GPa} \\ \bar{G}_{xy} &= 13,5 \text{ GPa} \end{aligned} \right\} (15)$$

These values enabled preliminary skin thickness estimates, after which lamination theory was used to calculate more exact in-plane stiffnesses. The relatively large value of E/\bar{E}_x did not result in excessive model skin thicknesses. Using Eqns. (13) and (15), the stiffness/strength advantage of the carbon material was estimated as⁽⁷⁾

$$(E/\bar{E}_x)(S_{11}/S) = (72,5/38,9)(950/460) = 3,85 \quad (16)$$

Plywood properties were estimated in a similar way, using test data⁽⁸⁾, as

$$\bar{E}_{\text{ply}} = 3,88 \text{ GPa}, \quad \bar{G}_{\text{ply}} = 1,44 \text{ GPa} \quad (17)$$

Verification of Material Properties

Before proceeding with the model design it was necessary to confirm calculated laminate properties. For this purpose three simple beam structures were built, all of which were rectangular in section. Two of them were straight single cell carbon structures, differing only in their layup schemes, and were used to check calculated EI and GJ values. The third beam was a tapered two-cell structure built of carbon and plywood. It was used to check deflections calculated by FE analysis. Measured and calculated bending and torsional stiffnesses for beams 1 and 2 agreed to within ~5%, while the deflections for beam 3 were within 5 to 10%.

Model Sizing

Sizing of the model structure was done primarily on a section by section basis. Bending and torsional stiffnesses and shear centre locations were matched as closely as possible at the selected wing stations. Steps in thickness between stations were accommodated by adding or dropping plies approximately halfway between the stations. Only layup angles of 45°, -45°, 0° and 90° were used, referenced to false spar 3, the approximate elastic axis. Laminates using these angles could be expected to have reasonably linear shear stress-strain behaviour, as they are not matrix dominated⁽⁹⁾. The skins were sized to provide the correct proportion of total bending stiffness (~95%). The major contribution to this stiffness comes from the Az² term (parallel axis theorem), so since geometry was fixed, and only skin thickness can vary

$$t_r \approx (EI_r)(1/L_r)^3(1/E_r) = 0,29 \quad (18)$$

Thus model skin thickness had to be approximately 0,29 of full scale thickness. Knowing the layed up thickness of the 6104 material enabled calculation of the number of plies required in each skin patch. The problem was then to design a laminate that gave E₁₁ ≈ 39,0 GPa with the desired number of layers. Lamination theory was used iteratively for this. In the region between the rear spar and the flap deflector false spar (Figure 9) the bias was in favour of E₂₂ since this region supports the trailing edge. To avoid coupling specially orthotropic laminates were used. As an example, final model skin patches for the top skin are shown in Figure 7, in which the number of plies in each patch is indicated. The selected layups are unusual in that they are anti-symmetric. Such layups offer greater freedom in achieving specially orthotropic properties⁽¹⁰⁾. E₁₁ and E₂₂ values ranged from ~31 to 41 GPa, while G₁₂ values were between ~11,5 and 16,8 GPa.

Once the skins were finalised, spars were selected to bring bending and torsional stiffnesses up to the target values and to locate the shear centre of each section. This was done iteratively using SECP, by varying the size, material and layup schemes. In practice two or three iterations were sufficient. Any one model section contained different laminates, so thicknesses were normalised to a reference value by introducing an appropriate modulus ratio n = E/E₀ for bending or m = G/G₀ for torsion, and modifying actual thicknesses in this same ratio. Final spar thicknesses varied from 0,80 to 3,20 mm.

Ribs were not scaled as such, but were sized to keep their relative proportions and stiffnesses fairly similar to those of the full scale wing. Layup schemes for the

carbon ribs were chosen such that their torsional stiffnesses were quite high, at the expense of bending stiffnesses. Rib thicknesses varied between 0,60 and 2,50 mm. Figure 2 shows the comparison between calculated and target stiffnesses and shear centre locations across the span for the final model structure.

The main root fitting is an important part of the structure, as all the bending loads pass through it. In scaling this fitting, which was done separately to the rest of the structure, only transverse bending stiffness was matched since torsional and in-plane loads are reacted by the secondary fore and aft attachments. 2024-T3 aluminium was used to match the full scale steel part, thus enabling easily machinable thicknesses to be obtained. The model fitting was kept geometrically similar to full scale, but simpler. A schematic of the model fitting, which was cut on a 3-axis NC machine, is shown in Figure 8.

Modelling of the launcher and store required a different approach. These components were designed using GVT results and overall measured mass properties, on the assumptions (a) they are uniform beams, (b) rotary inertia, shear deformation and axial loads are unimportant and (c) only the first transverse mode of each component need be simulated. The equation describing the lateral vibration is⁽¹¹⁾

$$\frac{\partial^2 u}{\partial t^2} + \left(\frac{EI}{m}\right) \frac{\partial^4 u}{\partial x^4} = 0 \quad (19)$$

which for free-free boundary conditions (as for the GVT's) has the solution

$$\cos(\beta l) \cosh(\beta l) = 1 \quad (20)$$

The first root of Eqn. (20) is given by

$$\beta_1 = 4,730041/l = (m\omega^2/EI)^{0,25} \quad (21)$$

Eqn. (21) enabled estimates of beam bending stiffnesses to match the first measured modes. After appropriate scaling of these values model components were designed (with cruciform cross-sections) using Newton-Raphson iteration. Mass properties were matched by adding two point masses such that overall mass, centre of gravity (cg) and mass inertia about the cg were correct. The launcher was made hollow to meet mass requirements.

MODEL STRUCTURAL LAYOUT

In applying the previously described design procedures, a similar, but simplified structural layout to that of the full scale wing was chosen. The main reasons for this were (a) to maintain as closely as possible the balance between skins and internal structure, (b) to build an efficient structure so as not to exceed mass allowances and (c) to simulate load paths properly. It was originally intended to reduce by approximately 50% the number of spars and ribs in the model, compared with the full scale wing. However, in performing the design iterations, and to satisfy points (a) and (c) above, this was found unrealistic.

The final skin layups for the main structural box are summarised in Figure 7 and Table 4. All skin plies were kept continuous except the centre ply, which was orientated at 0° in all laminates with 15 layers or more, otherwise at 90°. The outer two layers (inside and outside) of each skin were continuous over the whole

structural box, as can be seen from Table 4. As the model has no control surfaces, its leading and trailing edges are continuous. In order to add minimal stiffness to the main structural box, but to have adequate strength and buckling resistance, they comprised two layers of TORAYCA 6104/EPO 625 (top and bottom) orientated at 90° to false spar 3, supported by a lattice grid milled from microballoon. The resulting structure is soft spanwise, but stiff and strong chordwise.

Figure 9 shows the internal structure, in which the relatively large number of spars and ribs is evident. Between the root rib and rib 3, only false spar 4 was dropped, but from rib 3 to rib 4, false spars 1, 2, 4 and 5 were dropped. Outboard of rib 4 thin stiffeners were introduced to support the skin and help transfer store loads to the main structural box. The full size wing has relatively few ribs, and all except one (rib 2A) were maintained. The front, rear and parts of false spars 2 and 3, as well as ribs OC, 1 and 3, were made as TORAYCA 6142 carbon channel sections. All other spars and ribs were either birch ply or foam, as summarised in Table 5 and Figure 9.

Mounting and store attachment fittings were included in the model such that load paths were properly represented. With the exception of the main root attachment (Figure 8) their detail design was not copied from full scale. The main root fitting was made from 2024-T3 aluminium, the pylon attachments and secondary root fittings from BS15 aluminium or cotton flocks, with threaded steel inserts, and the launcher attachments from mild steel.

MODEL CONSTRUCTION

Skin ply patterns were marked on the moulds, so templates could be made and the plies cut out. Each skin, including leading and trailing edge, was hand layed-up wet and cured under vacuum. Once cured, they were NOT removed from the moulds until the model was completed. Internal carbon structures were also wet hand layups, and were pressed in male/female moulds derived from microballoon printouts taken from between the skins. This ensured a perfect fit whilst allowing for a 0,15 mm bondline, without having to know exact skin thicknesses⁽¹²⁾.

Plywood parts were hand-shaped, using printouts as templates, whilst the metal parts (including the launcher and store) were NC or hand-machined as appropriate. All joints in the model were bonded using CIBA GEIGY REDUX 410 or quickset epoxy. Such joints had previously been tested and found adequate.

The aluminium launcher and store simply bolted to the wing tip with high strength M4 cap screws. The launcher attaches to the wing at two points, and the store to the launcher at three points. It is likely that the store/launcher interface will have to be improved.

When the structure itself was completed and weighed, mass distribution calculations were finalised and ballast masses added as required. These lead masses were shaped to fit between the top and bottom skins, and bonded in place. The moulds were then closed to complete the model, with cotton flocks being used to simultaneously fill and bond the leading and trailing edges and wing tip, and pot in the launcher attachments.

A special mounting bracket was manufactured to attach the model to a backstop for static and vibration tests. As there was no reference point to work from, each

component of the mount system was made separately, thus ensuring easy alignment. All mounting pins were press fits to exclude free play.

MODEL CALIBRATION

Calibration tests are required to check the validity of the model and to set limits for static and dynamic loads in order to avoid over-stressing the model during tunnel tests. Model calibration essentially consists of completing the following (not necessarily in the given order):

- a) Define an upper load limit, for example calculated steady aerodynamic loads at 2° incidence.
- b) Test the model to these loads and measure deflections and strains, calibrating suitably located strain gauge bridges in the process.
- c) Perform static load-deflection tests as done for the full scale wing, using correctly scaled loads, and reduce the data appropriately.
- d) Vibrate the model to high load levels to obtain the limit for dynamic loading, using the strain gauge bridges, or installed miniature accelerometers to monitor these loads. This test is to some extent inter-related with (a) and (b), and some iteration may be necessary.
- e) Perform mass and inertia calibration of the launcher and store. Do a GVT on them both individually and as a unit and correct them as necessary to match target values.
- f) Perform GVT's on the model, for both clean wing and tip store configurations.
- g) Swing the model on a pendulum to obtain pitch, roll and yaw inertias, and locate the centre of gravity.
- h) Make adjustments to the model (stiffness and mass) and repeat tests as necessary.
- i) Cut the model into strips, then blocks, and measure its actual mass and inertia.

Based on model calibration results, the FE model must be tuned and structural redesign required for the second model completed.

Preliminary Calibration Results

At this time, only limited tests have been done with the model. The results obtained are considered good, but need verification. Indications are that the model is a little too stiff, especially in torsion, and too heavy. Briefly, some selected results are:

Mass Properties:

Target mass = 6504 g
Measured mass = 6587 g (+1,26%)

Target cg(x;y) = (178,8; 414,1) mm
Measured cg(x;y) = (178,0; 405,7) mm (-0,4; -2,1)%

(x,y given with respect to intersection of aircraft centre line and frame 25 - see Figure 1).

Static Tests:

Results for a tip bending (up) static load test are given in Table 6 and Figure 5. For this test, equal loads were applied at points L1 and L2, and deflections measured at points 19 and 21 (Figure 9). From Figure 5 it can be seen that this particular test showed bending stiffness to be ~5-6% high and torsional stiffness ~11-12% high, figures confirmed by the model GVT. Figure 5 also shows the linear behaviour of both full scale and model wings.

Launcher and Store frequency scans:

Scans of the launcher and store yielded the following frequencies for the first transverse bending modes.

Launcher:	Target = 246,6 Hz
	Measured = 264,4 Hz (+6,4%)
Store:	Target = 157,5 Hz
	Measured = 226,9 Hz (+30,6%)
Launcher/Store:	Target = 149,7 Hz
	Measured = 205,0 Hz (+27,0%)

Since mass and inertia properties of both launcher and store were correct, stiffnesses were obviously over-estimated, and will have to be corrected.

Clean Wing Ground Vibration Test:

Using impact testing, the first five modal frequencies of the clean wing were measured, and mode shapes for the first three modes extracted. Model frequencies were within 5% of target values, as shown in Table 7. Model mode shapes and node lines agreed well with full scale, except the node line for first torsion, which does not sweep back sharply at the tip as in the full scale structure. This can be seen clearly in Figure 3, and is probably due to the absence of an aileron in the model.

Wing plus Tip Store Ground Vibration Test:

Good results were again obtained for this configuration as can be seen from Table 8 and Figure 4. Modal frequencies were within 5%, except for the first torsion mode, which was 7% high. This is thought to be due to excessive stiffening effect of the launcher/store combination. Launcher and store stiffnesses will be varied, and the effect of this on wing torsion established, using the FE model as a guide. Mode shapes for the first four modes agree closely. Third bending and second torsion mode shapes, however, are not as good, although not completely wrong. These modes have relatively large control surface contributions (especially second torsion) and are therefore unlikely to be well represented by this model.

CONCLUSIONS

The design and construction of the first (calibration) Mach scaled flutter model wing has been completed. Great care was taken in properly simulating load paths and in the design of the root mounting, as it is especially important in simulating the first bending mode. The basic structure was easily built well within mass limits. Preliminary calibration results show the model's elastic and dynamic behaviour to be representative of the full scale wing, and within normally accepted limits. They must, however, be verified by further more detailed testing. These good results are encouraging, especially in that (a) carbon composites have been used to simulate a metal wing, (b) it is the first attempt at DAST to design and build such a model, and (c) relatively simple design procedures were used for the preliminary analysis, so the physics was not lost in mathematics.

Based on the results of these and further detailed calibration tests, the maths model will be tuned and used more extensively in the redesign of a second model, to be used for actual wind tunnel flutter testing.

REFERENCES

1. Yoo, C.H. : Cross-Section Properties of Thin Walled Multi-Cellular Section, Computers and Structures, Vol. 22, No. 1, 1986.
2. Dongarra, J.J., Moler, C.B., Bunch, J.R. and Stewart, G.W. : LINPACK Users Guide, pp. 9.1-9.25, Society for Industrial and Applied Mathematics, Philadelphia, 1979.
3. Van den Broek, G.J. : NIAST Report 87/90, June 1987, CSIR, Pretoria, RSA.
4. Schrem, E. : Summary of PERMAS Version 2.0, Tech. Note, 3 Nov. 1986, INTES, GmbH, Stuttgart.
5. Parisch, H. : The QUAD4 Shell Elements in PERMAS, User Manual, INTES, publication 402, PEVA, Stuttgart, 1985.
6. Jones, R.M. : Mechanics of Composite Materials, Scripta Book Company, 1975.
7. McCullers, L.A. and Naberhaus, J.D. : Automated Structural Design and Analysis of Advanced Composite Wing Models, Computers and Structures, Vol. 3, 1973.
8. Liebenberg, D. : The Mechanical Properties of Plywood, NIAST Report 86/71, June 1986, CSIR, Pretoria, RSA.
9. Ekstrom, C.V. and Spain, C.V. : Design Considerations and Experiences in the use of Composite Material for an Aeroelastic Research Wing, AIAA paper 82-0678.
10. ESDU Item 82013, Laminar Stacking Sequences for Special Orthotropy, (Application to fibre semiferred composites).
11. Tse, F.S., Morse, I.E. and Hinckle, R.T. : Mechanical Vibrations : Theory and Application, 2nd ed., Allyn and Bacon, 1978.
12. Sutherland, A.P.N. : NIAST Report 88/79, CSIR, Pretoria, RSA.
13. Cole, S.R., Rivera, J.A. Jr. and Nagaraja, K.S. : Flutter Study of an Advanced Composite Wing with External Stores, AIAA paper 87-0880.

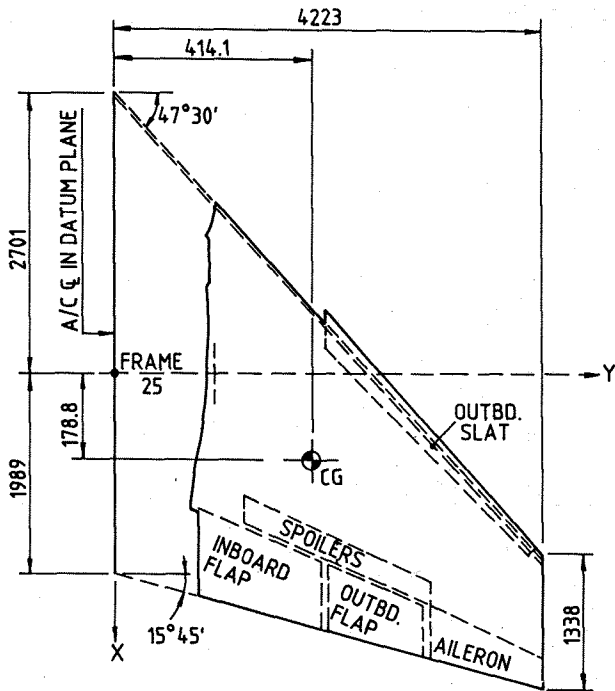


Figure 1 : Wing planform geometry - full scale.

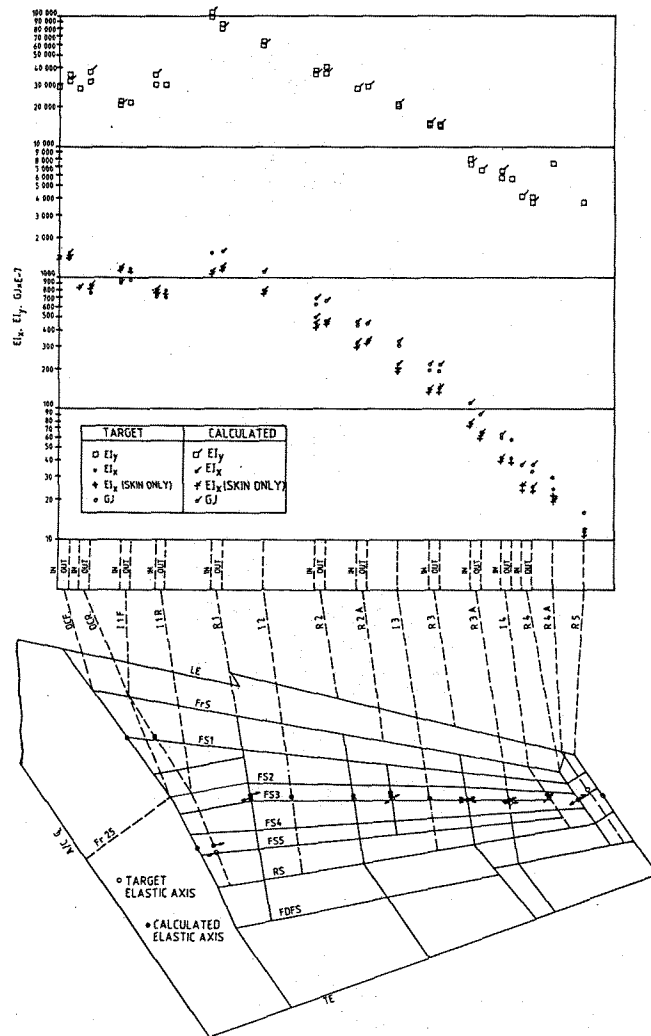


Figure 2 : Model target and calculated sectional properties.

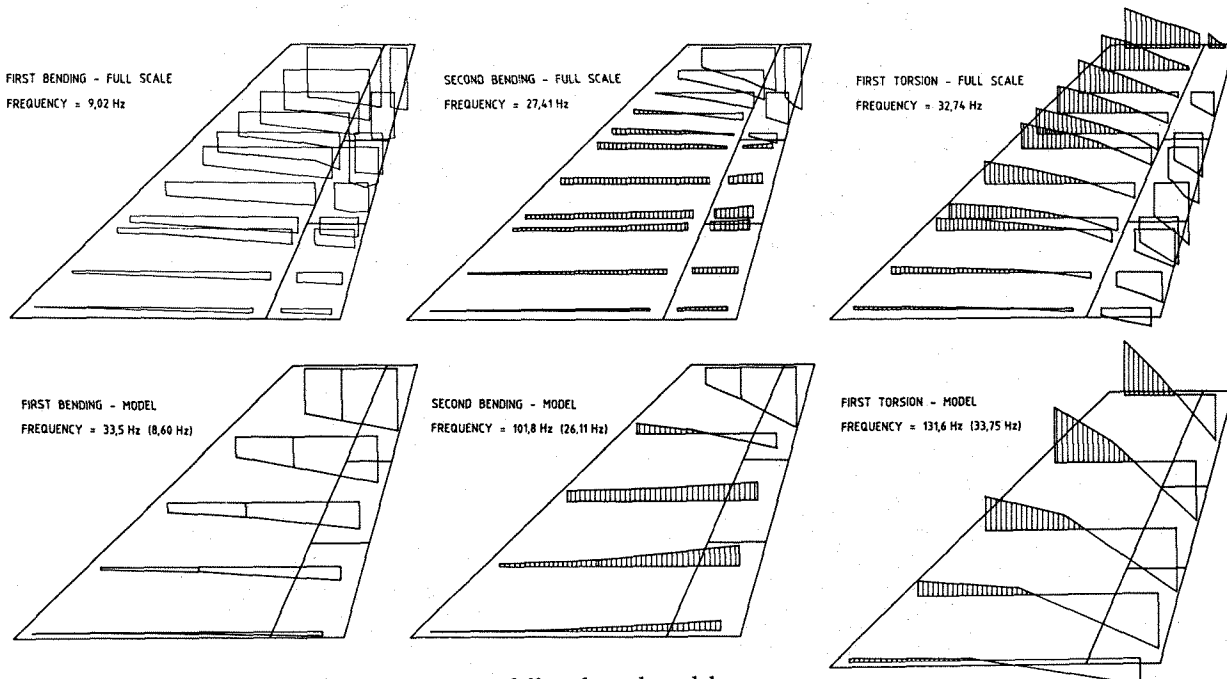


Figure 3 : Selected modes : clean wing - full scale and model.

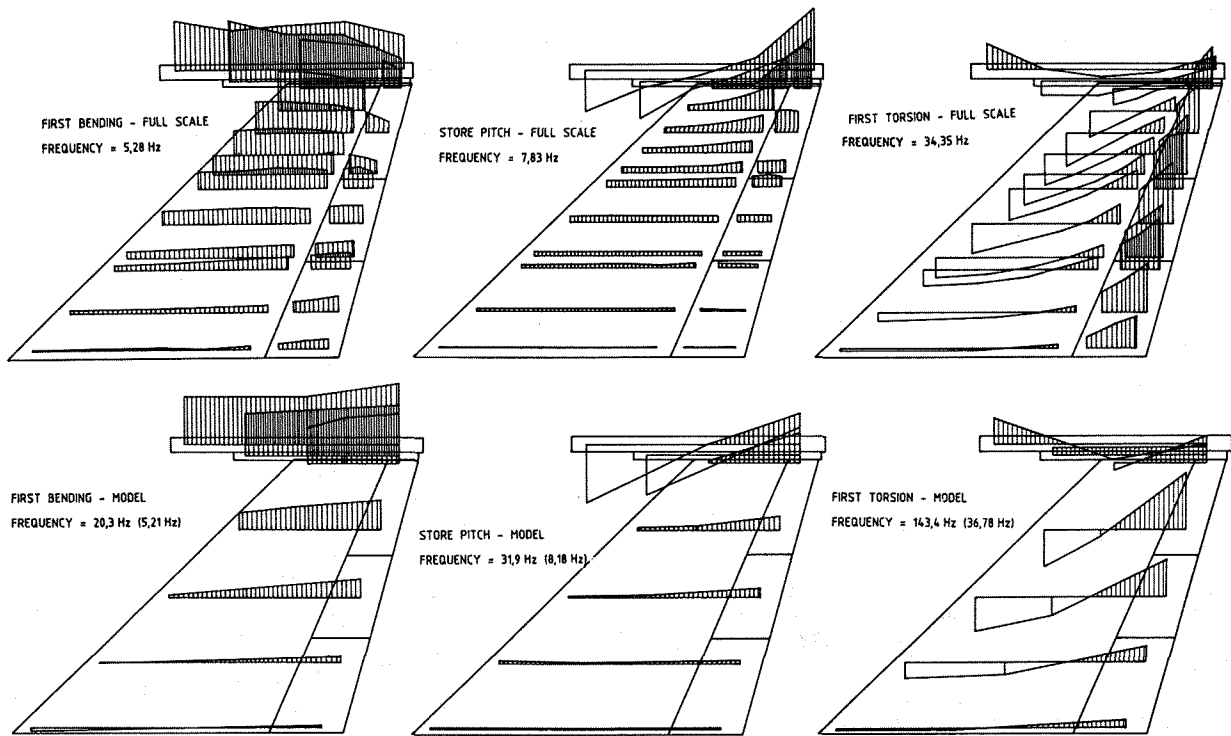


Figure 4 : Selected modes : wing with tip store - full scale and model.

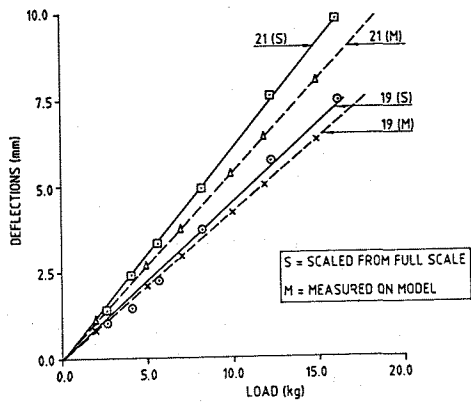


Figure 5 : Scaled deflections vs. load, points 19 and 21.

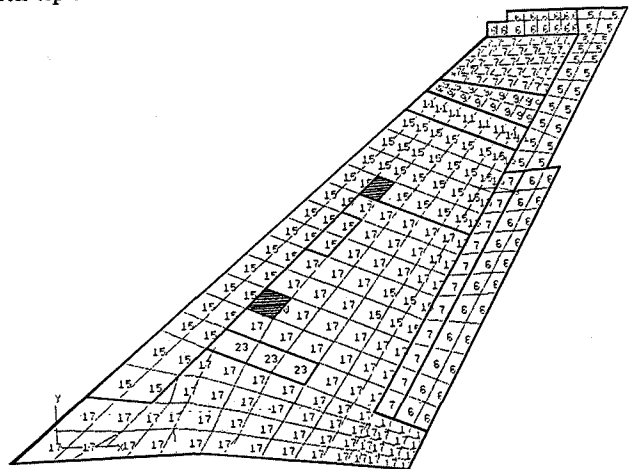


Figure 7 : Top skin patch laminates selected for model.

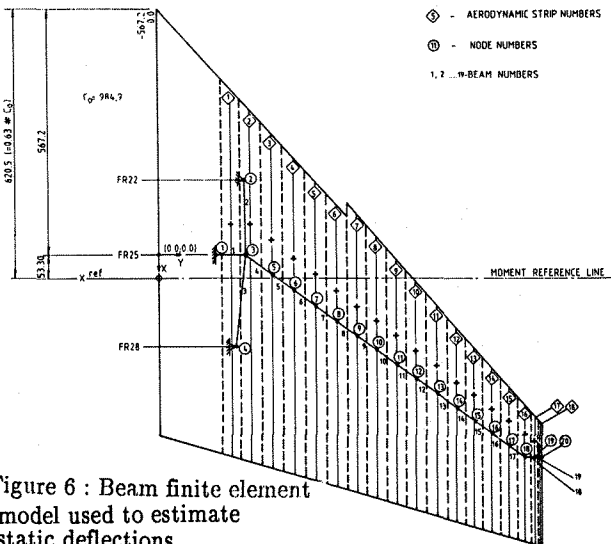


Figure 6 : Beam finite element model used to estimate static deflections.

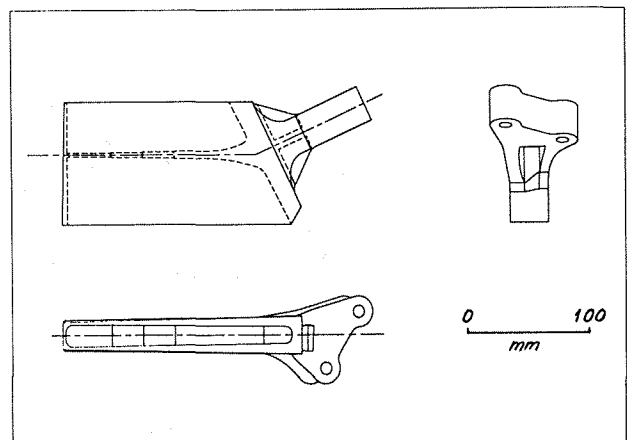


Figure 8 : Model main root fitting.

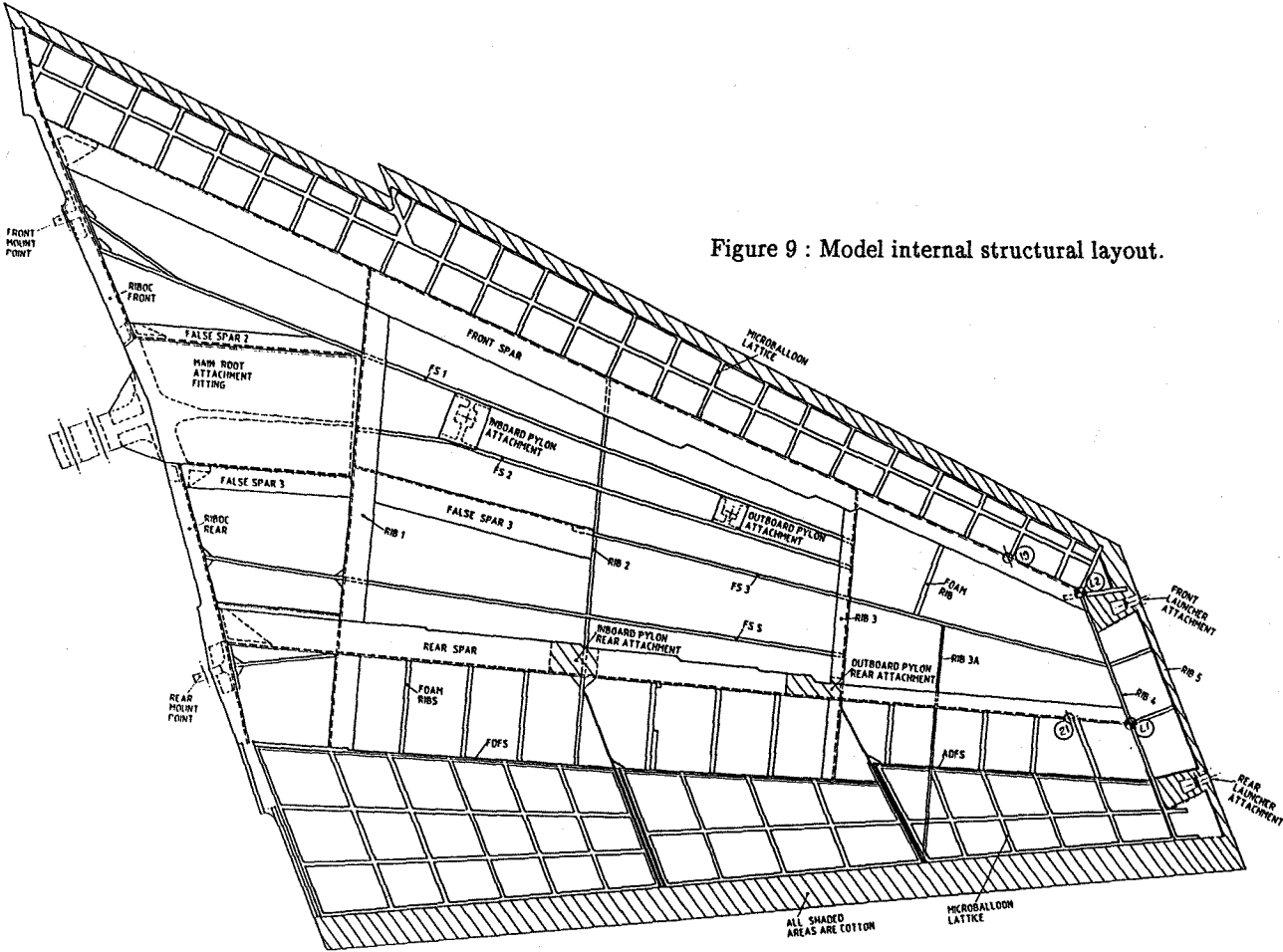


Figure 9 : Model internal structural layout.

Table 1 : Modal properties of full scale wing - clean configuration.

MODE NO.	FREQ. (Hz)	DAMP-ING	CALC. MODAL MASS (kgcm ²)	MODAL DESIGNATION
1	9,02	0,0084	45,91	First bending
2	27,41	0,0072	6,39	Second bending
3	32,74	0,0051	22,14	First torsion

Table 2 : Modal properties of full scale wing - launcher plus store configuration.

MODE NO.	FREQ. (Hz)	DAMP-ING	CALC. MODAL MASS (kgcm ²)	MODAL DESIGNATION
1	5,28	0,0112	86,73	First bending
2	7,83	0,0074	21,99	Store pitching
3	17,75	0,0052	24,47	Second bending
4	34,35	0,0071	36,86	First torsion
5	37,22	0,0076	28,29	Third bending
6	43,03	0,0068	32,85	Second torsion

Table 3 : Launcher and store frequencies (first bending).

COMPONENT	MODAL FREQUENCY (Hz)	
	TRANSVERSE	IN-PLANE
Launcher	63,5	78,2
Store	40,4	40,4

Table 4 : Selected skin laminates - layup schemes.

NO. OF LAYERS	THICKNESS (mm)	LAYUP SCHEME
5	0,85	-45/45/90/-45/45
6	1,02	-45/45/90/0/-45/45
7	1,12	-45/45/0/90/0/-45/45
9	1,44	-45/45/0/45/90/-45/0/-45/45
11	1,68	-45/45/0/90/45/0/-45/90/0/-45/45
15	2,25	-45/45/90/0/90/45/-45/0/45/-45/90/0/90/-45/45
17	2,55	-45/45/90/0/90/45/-45/0/0/45/-45/90/0/90-45/45
19	2,85	-45/45/90/0/90/45/-45/0/0/45/-45/90/0/90/-45/45
23	3,45	-45/45/0/90/90/90/0/90/45/-45/0/0/45/-45/90/0/90/90/0/-45/45

Table 5 : Spars and ribs construction.

COMPONENT	MATERIAL	THICKNESS (mm)	LAYUP SCHEME
Front spar:			
OC → 1 *	6142/EPO625	1,50	45/45/45/45/0/45/45/45/45
1 → I2+ ⊙	6142/EPO625	1,50	45/45/45/45/45/45/45/45/45
I2+ → 2A+	6142/EPO625	1,20	45/45/45/0/45/45/45
2A+ → 4	6142/EPO625	0,80	45/45/0/45/45
False spar 1:			
OC → 1 *	Birch ply	3,20	-
1 → 3	Birch ply	2,50	-
False spar 2:			
OC → 1 *	6142/EPO625	1,50	45/45/45/45/0/45/45/45/45
1 → 3	Birch ply	2,50	-
False spar 3:			
OC → 1	6142/EPO625	1,50	45/45/45/45/0/45/45/45/45
1 → 1+	6142/EPO625	1,50	45/45/45/45/45/45/45/45/45
1+ → I2+	6142/EPO625	1,20	45/45/45/0/45/45/45
I2 → 2	6142/EPO625	0,80	45/45/0/45/45
2 → 4	Birch ply	2,50	-
False spar 5:			
OC → 1 *	Birch ply	3,20	-
1 → 3	Birch ply	2,50	-
Rear spar:			
OC → 1 *	6142/EPO625	1,50	45/45/45/45/0/45/45/45/45
1 → I2+	6142/EPO625	1,50	45/45/45/45/45/45/45/45/45
I2+ → 2A+	6142/EPO625	1,20	45/45/45/0/45/45/45
2A+ → 4	6142/EPO625	0,80	45/45/0/45/45
FDFS:			
OC → 1	Birch ply	3,20	-
1 → 4	Birch ply	1,00	-
Rib OC	6142/EPO625	1,50	45/0/0/45/45/45/0/0/45
Rib 1	6142/EPO625	1,20	45/0/0/45/0/0/45
Rib 2	Birch ply	2,50	-
Rib 3	6142/EPO625	0,60	45/0/45
Rib 3A	Birch ply	1,50	-
Rib 4	Birch ply	2,50	-
Rib 5	Birch ply	1,50	-

* OC → 1 = Rib OC to Rib 1 ⊙ I2+ = halfway between I2 and next section, etc.

Table 6 : Static test results - tip bending (up).

DISPLACEMENTS (mm)					
POINT ↓	LOAD LEVEL →	0,25	0,50	0,75	1,00
19	Target	1,75	3,73	5,52	7,41
	Actual	1,68	3,50	5,23	7,00
	Ratio	0,96	0,94	0,95	0,94
21	Target	2,34	4,95	7,50	9,85
	Actual	2,21	4,50	6,70	8,85
	Ratio	0,94	0,91	0,89	0,90

Table 7 : Model GVT results - clean wing.

MODE NO.	FREQUENCY (Hz)			MODE DESIGNATION
	TARGET	MEASURED	RATIO	
1	35,2	33,5	0,95	First bending
2	106,9	102,0	0,95	Second bending
3	127,7	131,5	1,03	First torsion
4	204,6	196,6	0,96	Third bending
5	Not measured	227,0	-	Second torsion

Table 8 : Model GVT results - tip store configuration.

MODE NO.	FREQUENCY (Hz)			MODE DESIGNATION
	TARGET	MEASURED	RATIO	
1	20,6	20,3	0,99	First bending
2	30,5	31,9	1,05	Store pitch
3	69,2	69,7	1,01	Second bending
4	133,9	143,3	1,07	First torsion
5	145,1	150,1	1,03	Third bending